View metadata, citation and similar papers at core.ac.uk

brought to you by CORE

provided by Repository@Hull - CRIS

Manuscript: Yip et al, "A cholesteric liquid crystal device having stable uniform lying helix structure"

A cholesteric liquid crystal device having stable uniform lying helix structure

W. C. Yip[1], Chris Welch[2], Georg H. Mehl[2] and Timothy D. Wilkinson[1]

[1]*Department of Engineering, University of Cambridge, 9 JJ Thomson Avenue, Cambridge, CB3 0FA, UK.*

[2]*Department of Chemistry, University of Hull, Hull, HU6 7RX, UK.*

Author for correspondence: larry.wc.yip@ieee.org

Abstract

A cholesteric liquid crystal device having the uniform lying helix (ULH) structure shows stable and reversible characteristics and it has been demonstrated for the analogue modulation in 10 micro-second response time at room temperature. The device comprises a polymer-free chiral nematic liquid crystal mixture and the photoalignment layer is irradiated by the UV light to cause a preferred orientation of the liquid crystal. The ULH structure is obtained by cooling the liquid crystal mixture from the isotropic phase transition temperature in the presence of electric field. On the electrical and thermal cycling, no noticeable hysteresis has been observed. In addition, the tilt angle and response time have been measured in good agreement with Meyer's theory on the flexoelectric effect in liquid crystals.

1. Introduction

In 1969, Meyer discussed theoretically the splay-bend deformation of liquid crystals in association with an electric polarization. He further derived the linear electro-optic equation in liquid crystals assuming the negligible dielectric anisotropy [1]. In case of cholesteric liquid crystal, the rotation of optics axis has been predicted giving rise to a tilt angle when an electric field is applied normal to the optics axis. The optics axis is parallel to the helix axis of cholesteric liquid crystal in the absence of electric field. For small rotation, this tilt angle is linearly dependent on the magnitude of electric field. In addition, the sign of tilt angle follows the polarity of electric field. Interestingly, the response time does not depend on the electric field in small rotation approximation. It is commonly referred to as the flexoelectric effect. This effect has been observed in the nematic, cholesteric and smectic phases particularly in the wedge shape or bend core liquid crystal molecules.

In case of small dielectric anisotropy, a field-induced domain pattern containing regions of splay and bend could be theoretically formed in nematic liquid crystals. The domain width has been suggested to be inversely proportional to the magnitude of electric field and the $\bar{e}/K_1$ ratio. The mean flexoelectric coefficient and the splay elastic constant are denoted by $\bar{e}$ and K_1 respectively. So, the domain width can be large since $\bar{e}/K_1$ is usually small. This is conditioned on the identical flexoelectric coefficients, one elastic constant approximation and negligible current effects. It was further discussed by Patel and Meyer that the formation of a continuously rotating director structure in alternating bands of splay and bend deformation could be observed in cholesteric liquid crystal [2]. Because the director is already continuously rotating in the cholesteric in a pure twist fashion. The formation will be manifested readily as the flexoelectric effect becomes non-negligible. Later in 1989, Patel and Lee [3] measured the response time about 100μs for the ULH structure in cholesteric liquid crystal. It agreed with the predicted value of 10-100μs. This fast response time which was also predicted to be independent of the electric field for small rotation was shown experimentally.

The problem to obtain a stable and homogeneous ULH structure has been reported since the late eighties. Often, it requires cooling the liquid crystal from the isotropic phase in the presence of electric field to obtain the ULH structure. Mechanical shearing has been described in some occasions necessary for the homogeneity of ULH structure. To minimize the elastic energy associated with the distortion, the ULH structure in homogeneous or homeotropic boundary condition has been found not stable. It will relax back to the Grandjean texture after the removal of electric field. Attempts such as polymer network in the bulk of liquid crystal or at the substrate surface had been demonstrated to stabilize the ULH structure [4-5]. The polymer-stabilized ULH structure can be restored in the thermal cycling from isotropic phase to cholesteric phase. It was also stable for the electric field greater than the helix unwinding field. There were issues not yet solved such as hysteresis problem and retarded response time although the progress in minimizing the residual birefringence has been made.

Stabilization by the grating structures with periodic anchoring conditions [6], periodic microchannels [7], surface relief structures generated by laser [8] and by moulding [9] were also reported. The issue associated with these techniques was the low fill factor since the grating structure occupied part of the footprint for the optical modulation. Other techniques such as shearing [10], treatment by plasma beam [11], cholesteric alignment layer [12], inhomogeneity induced by in-plane field [13-14] and dynamic state switching [15] were found favourable to the formation of stable ULH structures. However, stabilization of the ULH structure by shearing [10] would not be compatible with present LCD manufacturing processes. Treatment by plasma beam [11] provides questionable homogeneity over a large area and it is considered to be incompatible with present LCD manufacturing processes. Stabilization of the ULH structure by the incorporation of cholesteric alignment layer [12] has the

disadvantage that a sizeable thickness of cholesteric alignment layer is required. This causes problems such as voltage drop, voltage holding ratio and residual birefringence. Inhomogeneity induced by in-plane field [13-14] has the possibility of stabilizing the ULH structure. Nevertheless, this provides a limited fill factor due to the requirement for the interdigitated electrodes. Stabilization of the ULH structure by dynamic state switching [15] has the drawback that a periodic reset is required to refresh the ULH structure and the stability at an elevated temperature is not clear.

2. Theory

For the flexoelectric effect in cholesteric liquid crystals, we recall the equations derived by Patel *et al* [2, 3] and use the same notations. In the following discussion, the uniform lying helix (ULH) structure is referred to the topological structure formed in cholesteric liquid crystal wherein the helical axis is lying parallel to the substrate surface. In the presence of electric field, the helical axis of ULH structure is rotated by a tilt angle φ about the x-axis. It is assumed that the helix axis of ULH structure is initially along the z-direction. The electric field E is applied in the x-direction while the director of cholesteric liquid crystal is parallel to the x-y plane. The equilibrium helical distortion is determined by the balance between the elastic energy and the field energy due to the flexoelectric coupling with the electric field under the assumption of non-negligible dielectric contribution. Therefore, taking the one elastic constant approximation and for small rotation, the tilt angle is given by

$$tan(\emptyset) = \bar{e}E/t_0K_1 \quad (1)$$

where K_1 is the splay elastic constant, t_0 is the equilibrium twist of cholesteric liquid crystal and $\bar{e}$ is the mean flexoelectric coefficient assuming that $\bar{e}=e_s=e_b$. The splay and bend flexoelectric coefficients are denoted by e_s and e_b respectively. The equilibrium twist is defined as $2\pi/p_0$ where p_0 is the corresponding pitch of cholesteric liquid crystal at equilibrium. The electric field represented by E is homogeneous spatially in this case. In addition, according to the balance of torque equation that governs the dynamics of helix rotation, the characteristic time for small rotation is given by

$$\tau = \gamma_1/t_0^2K_1 \quad (2)$$

where γ_1 is the viscosity of pure rotation. It is independent of electric field and it is measured as the average of rise time and fall time. It is commonly referred to as the response time. When the elastic constants are not equal, Rudquist *et al* [16] have obtained the following equation for the tilt angle in small rotation approximation.

$$tan(\emptyset) = \bar{e}E/t_0K_2 - \left[(K_1 + K_3)/2K_2 - 1\right]sin(\emptyset) \quad (3)$$

where K_2 and K_3 are the twist and bend elastic constants respectively. Since the tilt angle is usually small, Eq. (3) can be reduced to Eq. (1) with K_1 substituted by the average of K_1 and K_3. In the first order approximation, the authors have also replaced the splay elastic constant in Eq. (2) by the average of K_1 and K_3 to calculate the response time. So, we shall use the average of K_1 and K_3 to substitute K_1 accordingly.

3. Experiments

To measure the tilt angle and the response time, the device having the ULH structure was placed between the cross polarizers in an optical microscope. A coloured glass long-pass filter cut-off at 610nm was inserted in the light path. The choice was to compare the measurements by the Helium-Neon laser. The transmitted intensity and its relative change in term of the incident intensity I_0 are respectively given by

$$I = I_0 sin^2(2\beta) sin^2\left(\pi \Delta n d/\lambda_0\right) \quad (4a)$$

$$\Delta I/2I = sin(4\emptyset)/tan(2\beta) \quad (4b)$$

where β is the angle of optic axis relative to the polarizer axis in the absence of electric field. The effective birefringence, thickness of cell gap and centre wavelength of incident light are denoted by Δn, d and λ_0 respectively. At $\beta=22.5^0$, the tilt angle can be obtained by Eq. (1) and Eq. (4b). So, the relative change in transmitted intensity becomes proportional to four times of the electric field in small rotation approximation.

In Device 1, the transverse field switching electrodes were fabricated using the indium tin oxide (ITO) film. Azo-dye film was spin-coated on top of the transverse field electrode and it was baked at 80°C for 15min. The azo-dye material was patented and the experimental results can be found in the report by Yip *et al* [17]. It was exposed in proximity to a linearly polarized UV light at 5J/cm^2. A quartz photo-mask was used to transfer the image to the illuminated region. A polymer-free chiral nematic liquid crystal mixture comprising E7 and R5011 from Merck was disposed between the first and second substrates. Both substrates were made of glass material and the perimeter was sealed by Norland NOA 68 UV adhesives. An alternating electric field was applied while the liquid crystal was cooling from the isotropic phase. In this case, the electric field was homogeneous and substantially normal to the substrate surface. The ULH structure was observed to grow and after a sufficient long time it became stable in the absence of electric field.

In Device 2, the in-plane switching electrodes were fabricated using the aluminium on chromium film. Negative photoresist AZ nLOF 2020 from MicroChemicals was spin-coated at 4000rpm for 30 second before it was baked at 100°C for 1min. Then, it was exposed in proximity to UV light with a quartz photo-mask. It was post baked at 110°C for 1min before it was developed in AZ 726 MIF for 90 second. A layer of about 20nm chromium and 100nm aluminium was deposited in sequence by sputtering. Lift-off in 1-Methyl-2-pyrrolidon (NMP) and resist stripping by oxygen plasma were followed. At the end of the processes, the substrate having the electrodes for in-plane switching was obtained and it was substituted for the first substrate in Device 1. The in-plane switching electrodes were short-circuited externally by a connection wire. These were acted as the counter electrode when the electric field was applied in this case. Therefore, the electric field was not homogeneous spatially. Stable ULH structure was formed after the liquid crystal was cooling from the isotropic phase in the presence of electric field. For the normal operation, the connection wire would be removed and the ITO electrode on the second substrate would be left disconnected as a floating electrode.

In Device 3, the fringe field switching electrodes were fabricated using the materials of aluminium on chromium, silicon dioxide and ITO. To fabricate the first electrode, the ITO film was patterned by the lithographic technique and it was subsequently etched in diluted hydrochloric acid. A layer of 400nm silicon dioxide was then deposited by PECVD on top of the first electrode. The lithography, film deposition and lift-off steps for the second electrode were repeated according to Device 2. At the end of the processes, the substrate having the electrodes for fringe field switching was obtained and it was substituted for the first substrate in Device 1. The electric field was also not homogeneous spatially. To obtain the low threshold voltage and high breakdown field, high quality PECVD silicon oxide was critical. Stable ULH structure was formed as in Device 2 although there was fringe field induced inhomogeneity at the perimeter of electrode. Likewise, the ITO electrode on the second substrate would be floating for the normal operation. More information regarding the fabrication of these devices can be found in the published application [18].

The equipment used in these measurements were Olympus optical microscope BX 60, Hewlett Packard UV-visible spectroscopy system 8453, Agilent Technologies digital storage oscilloscope DSO5034A, Thurlby Thandar Instruments programmable function generator TG1304, Linkam hot stage LTS 350 with controller TMS 94, Thorlabs photo-diode PDA 55 and a calibrated high-voltage amplifier. It was noted that the measurements and the photo were taken at 22°C unless it was mentioned otherwise.

4. Results and Discussion

In a microscopic view, small domains were observed growing as the liquid crystal was cooling from the isotropic phase in the presence of electric field. These small domains coalesced and became large domains having a structure of long thin stripes. These large domains further grew to a ULH structure comprising aligned domains of splay and bend deformation. The ULH structure in the transverse field switching electrode configuration was aligned in a preferred orientation induced by the alignment layer. The azo-dye material was used for the alignment layer in this case. The ULH structure exhibited a very good homogeneity in a viewing area of 3mm x 4mm as shown in Fig. 1 (a)-(b). The azimuthal angle of optics axis relative to the polarizer axis was denoted by β whereas P, A and O denoted the polarizer axis, analyzer axis and optics axis respectively. In Fig. 1 (c)-(d), the width of long thin stripes was about 10μm whereas the typical length was longer than 400μm. The ULH structure comprising these aligned domains were found having stable and reversible characteristics. In a control experiment, this ULH structure can withstand cycling at a high electric field up to 10V/μm and high operating temperature close to 0.8 of the isotropic phase transition temperature.

According to our simulation results, the fluctuations in the surface director orientation and the discontinuous structural changes will be manifested at the substrate surfaces when the electric field reaches the cut-off condition at an elevated temperature below the isotropic phase transition temperature. Since the dielectric anisotropy is negligibly small in this regard, the flexoelectric effect becomes the dominant cause for the onset of aligned domain formation. It is also shown that the perturbation term in twist does not depend on the dielectric anisotropy and the continuous helical distortion will grow when the electric field is sufficiently large. On cooling down in the presence of electric field, the dielectric contribution begins to couple with the curvature induced by the flexoelectric effect and the ULH structure comprising the aligned domains of splay and bend deformation will be formed as a result. This is assumed that a flat surface without any protrusion is in direct contact with the liquid crystal layer. So, the rotating director in the form of splay and bend deformation is not perturbed locally by the surface distortion.

In Fig. 2, the ULH structure was obtained using a transverse field switching electrode configuration. Very good homogeneity at the azimuthal angle of 0° and 45° was observed in a viewing area of about 6mm in diameter. It was noted that the scattering of the non-illuminated background area was due to the formation of focal-conic texture. The device preparation was described in Device 1. In Fig. 3, the ULH structure was obtained using an in-plane switching electrode configuration and the device preparation was described in Device 2. The homogeneity was good in a viewing area of 600μm x 760μm as shown in the inserted photo. The in-plane electrodes were viewed dark at the azimuthal angle of 0° and 45° as shown in Fig. 3 (a) and Fig. 3 (b) respectively, since the photo was taken in the transmission mode. In Fig. 4, the ULH structure was obtained using a fringe field switching electrode configuration and the device preparation was described in Device 3. The homogeneity was reasonably good in a viewing area of 600μm x 760μm as shown in the inserted photo although there was a fringe field induced inhomogeneity at the perimeter of electrode. Likewise, the fringe field electrode shown in Fig. 4 (a) and Fig. 4 (b) was taken in the transmission mode. In Fig. 3 and Fig. 4, straight and parallel

metallic arrays were fabricated to form the comb-shaped electrodes and the electrode width and spacing were 10μm and 8μm respectively. In these figures, it was demonstrated that stable ULH structure can be formed in three types of electrode configuration each having a distinctively different spatial distribution of electric field.

These results were not obvious and they were not in agreement with other published work. Firstly, stable [13] and unstable [14] ULH structures had been inconsistently reported in the in-plane switching electrode configuration under the homogeneous boundary condition. Bimesogenic molecules of positive dielectric anisotropy and similar set of conditions were used. The authors attributed one of the causes to the inhomogeneity in the field produced by the interdigitated electrodes. Secondly, the commercial chiral nematic mixture was used in the homeotropic boundary condition to mitigate the difficulties in obtaining the ULH structure [14]. However, there was light leakage in both electrode and non-electrode regions shown in their results and the dark state was hardly homogeneous. It has been known that the rod-like liquid crystal molecules in proximity of an electrode region will have equal chance to orient in the left or right direction due to the symmetry of in-plane switching electrode structure. This happens regardless of the inhomogeneity in the field produced by the interdigitated electrodes. As a result, the liquid crystal molecules to a large extent cannot form a homogeneous observation in the electrode regions after the removal of electric field. This cannot be explained satisfactorily by the defects or randomly oriented domains of ULH formed simultaneously as the dominating causes for the observation. Therefore, we suggest that the dielectric coupling cannot be ignored according to our simulation results and it is the aligned domains inherited in our present work that stabilize the ULH structure after the removal of electric field. They can be formed under three distinctively different spatial distributions of electric field and they are resistant to the stress caused by the thermal and electrical field cycling.

To verify the observations, the measurements of tilt angle and response time were made and Device 1 was used for the largest possible fill factor and lower voltage requirement. The thickness of cell gap was estimated to be 4.2μm by analyzing the interference transmission spectrum. The triangle, square and circle represent the measurements at 10^0C, 20^0C and 30^0C respectively. The abbreviations "inc" and "dec" stand for the data measured on the incremental and decremental voltage cycle respectively. The dependence on tilt angle and response time at different temperature was plotted in Fig. 5 and the plots were linearly dependent on the square of electric field in agreement with Eq. (1) and Eq. (2). Taking the elastic constants K_1 and K_3 as 10.3pN and 15.8pN respectively, the mean flexoelectric coefficient $\bar{e}$ was determined to be 3.8pC/m by measuring the slope of plot at 20°C. It was assumed that the viscosity γ_1 was 0.3 Pa·s in this case. It was noted that the published data in the measurements of viscosity were scattered and the uncertainty may give rise to a possible error in the determination of mean flexoelectric coefficient. Accordingly, the pitch was deduced to be about 137nm which was difficult to be measured accurately by the spectral transmission method. The response time at different temperature was shown in Fig. 6 and the rectangular waveform at 1kHz was used. The rise time and the fall time were approximately equal and the response time was defined as an average. The response time was found independent of the electric field and the response time at 10^0C, 20^0C and 30^0C were measured as 20μs, 11μs and 7μs respectively. When the temperature was kept at 22^0C, the response time was equal to 10μs. The measurements of tilt angle and response time agreed with the predicted values [3]. So, it was concluded that the observations were due to the flexoelectric effect in liquid crystals.

5. Conclusions

In summary, we obtained the homogeneous ULH structure in three different electrode configurations that were stable and exhibited reversible characteristics on the electrical and thermal cycling. In addition, there was no noticeable change over a long period of time after the removal of electric field. As a matter of fact, we had stable samples on hand that were still functional according to this definition. We attributed this to the formation of aligned domains of splay and bend deformation. This enabled us to solve the long standing problem of stability and hysteresis particularly to meet the manufacturing requirements. Furthermore, the device had been demonstrated for the analogue modulation that showed the field-independent response time of 10 micro-second at room temperature and the linearly dependence of tilt angle on the electric field. These were in good agreement with Meyer's theory on the flexoelectric effect in liquid crystals.

Acknowledgments

Guangyu Yao was acknowledged to assist in the deposition of PECVD oxide. This work was based on the PCT application filed in 2017 by Yip *et al* that the ULH structure can be stabilized after the removal of electric field by the aligned domains of splay and bend deformation [18]. The project was funded by the Engineering and Physical Sciences Research Council in UK and the project number was EP/M016218/1.

Conflict of interest

The authors confirm that there are no known conflicts of interest associated with this publication and there has been no significant financial support for this work that could have influenced its outcome.

References

[1] Robert B. Meyer, Piezoelectric effects in liquid crystals, Phys. Rev. Lett. 22 (1969) 918-921.

[2] J. S. Patel and Robert B. Meyer, Flexoelectric electro-optics of a cholesteric liquid crystal, Phys. Rev. Lett. 58 (1987) 1538-1540.

[3] J. S. Patel and Sin-Doo Lee, Fast linear electro-optic effect based on cholesteric liquid crystals, J. Appl. Phys. 66 (1989) 1879-1881.

[4] P. Rudquist, L. Komitov and S. T. Lagerwall, Volume-stabilized ULH structure for the flexoelectro-optic effect and the phase-shift effect in cholesterics, Liq. Cryst. 24 (1998) 329-334.

[5] Sang Hwa Kim, Lei Shi and Liang-Chy Chien, Fast flexoelectric switching in a cholesteric liquid crystal cell with surface-localized polymer network, J. Phys. D 42 (2009) 195102.

[6] L. Komitov, G. P. Bryan-Brown, E. L. Wood and A. B. J. Smout, Alignment of cholesteric liquid crystals using periodic anchoring, J. Appl. Phys. 86 (1999) 3508-3511.

[7] Giovanni Carbone, Patrick Salter, Steve J. Elston, Peter Raynes, Luciano De Sio, Sameh Ferjani, Giuseppe Strangi, Cesare Umeton and Roberto Bartolino, Short pitch cholesteric electro-optical device based on periodic polymer structures, Appl. Phys. Lett. 95 (2009) 011102.

[8] Giovanni Carbone, Daniel Corbett, Steve J. Elston, Peter Raynes, Alexander Jesacher, Richard Simmonds and Martin Booth, Uniform lying helix alignment on periodic surface relief structure generated via laser scanning lithography, Mol. Cryst. Liq. Cryst. 544 (2011) 37-49.

[9] B. I. Outram, S. J. Elston, R. Tuffin, S. Siemianowski and B. Snow, The use of mould-templated surface structures for high-quality uniform-lying-helix liquid-crystal alignment, J. Appl. Phys. 113 (2013) 213111.

[10] Yo Inoue and Hiroshi Moritake, Formation of a defect-free uniform lying helix in a thick cholesteric liquid crystal cell, Appl. Phys. Express 8 (2015) 071701.

[11] Ruslan Kravchuk and Oleg V. Yaroshchuk, Alignment peculiarities of cholesteric liquid crystals on the surfaces processed by plasma beam, SID Symp. Dig. Tech. Papers 44 (2013) 1355-1358.

[12] G. Hegde and L. Komitov, Periodic anchoring condition for alignment of a short pitch cholesteric liquid crystal in uniform lying helix texture, Appl. Phys. Lett. 96 (2010) 113503.

[13] Damian J. Gardiner, Stephen M. Morris, Philip J. W. Hands, Flynn Castles, Malik M. Qasim, Wook-Sung Kim, Su Seok Choi, Timothy D. Wilkinson and Harry J. Coles, Spontaneous induction of the uniform lying helix alignment in bimesogenic liquid crystals for the flexoelectro-optic effect, Appl. Phys. Lett. 100 (2012) 063501.

[14] B. I. Outram and S. J. Elston, Alignment of cholesteric liquid crystals using the macroscopic flexoelectric polarization contribution to dielectric properties, Appl. Phys. Lett. 103 (2013) 141111.

[15] Chun-Ta Wang, Wei-Yuan Wang and Tsung-Hsien Lin, A stable and switchable uniform lying helix structure in cholesteric liquid crystals, Appl. Phys. Lett. 99 (2011) 041108.

[16] P. Rudquist, T. Carlsson, L. Komitov and S. T. Lagerwall, The flexoelectro-optic effect in cholesterics, Liq. Cryst. 22 (1997) 445-449.

[17] W. C. Yip, H. S. Kwok, V. M. Kozenkov and V. G. Chigrinov, Photo-patterned e-wave polarizer, Displays 22 (2001) 27-32.

[18] W. C. Yip and Timothy D. Wilkinson, Liquid crystal devices and method for manufacturing liquid crystal devices, World Intellectual Property Organization, WO2018192862 (2018).

Figure captions

Fig. 1 The ULH structure is formed in the transverse field switching electrode configuration where the aligned domains of splay and bend deformation in the absence of electric field are shown. Note: 1mm scale bar for (a)-(b) and 50μm scale bar for (c)-(d). The azimuthal angle β is 0° and 45° for (a) & (c) and (b) & (d) respectively.

Fig. 2 Large size ULH structure is formed homogeneously in the transverse field switching electrode configuration. Note: 1mm scale bar. The azimuthal angle β is 0° and 45° for the dark and bright states respectively.

Fig. 3 The ULH structure is formed in the in-plane switching electrode configuration. Note: 20μm scale bar (the inserted photo in 200μm scale bar). The azimuthal angle β is 0° and 45° for (a) and (b) respectively.

Fig. 4 The ULH structure is formed in the fringe field switching electrode configuration. Note: 20μm scale bar (the inserted photo in 200μm scale bar). The azimuthal angle β is 0° and 45° for (a) and (b) respectively.

Fig. 5 Plot of dependence on tilt angle and response time as a function of square of electric field at different temperature. The device in the transverse field switching electrode configuration was used for the measurements. Note: 10°C (Triangle), 20°C (Square) and 30°C (Circle).

Fig. 6 Plot of response time as a function of electric field at different temperature. The device in the transverse field switching electrode configuration was used for the measurements. Note: 10^0C (Triangle), 20^0C (Square) and 30^0C (Circle).

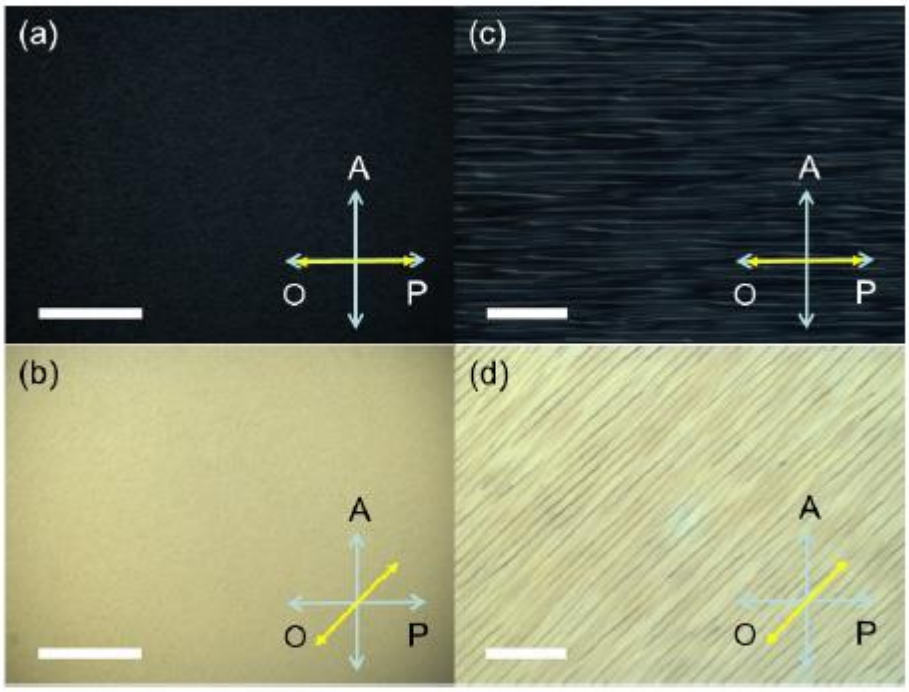

Fig. 1 The ULH structure is formed in the transverse field switching electrode configuration where the aligned domains of splay and bend deformation in the absence of electric field are shown. Note: 1mm scale bar for (a)-(b) and 50μm scale bar for (c)-(d). The azimuthal angle β is 0° and 45° for (a) & (c) and (b) & (d) respectively.

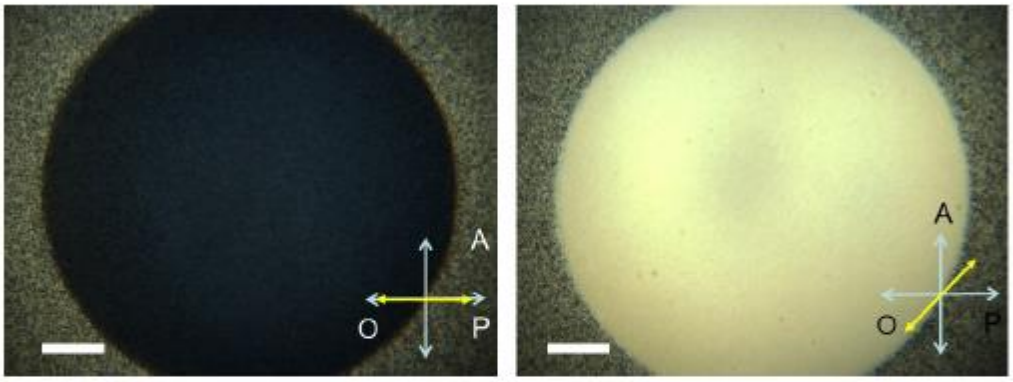

Fig. 2 Large size ULH structure is formed homogeneously in the transverse field switching electrode configuration. Note: 1mm scale bar. The azimuthal angle β is 0° and 45° for the dark and bright states respectively.

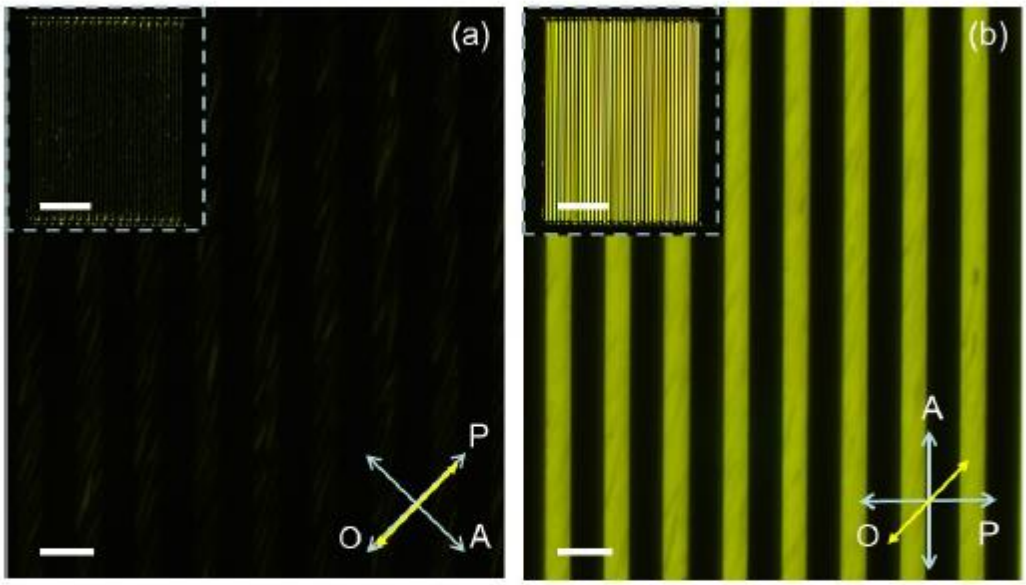

Fig. 3 The ULH structure is formed in the in-plane switching electrode configuration. Note: 20μm scale bar (the inserted photo in 200μm scale bar). The azimuthal angle β is 0° and 45° for (a) and (b) respectively.

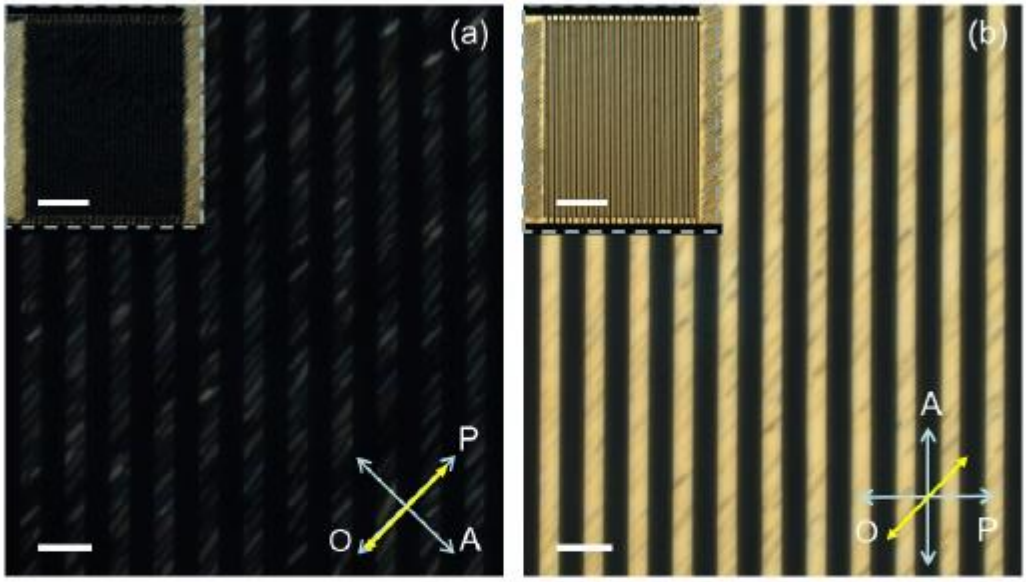

Fig. 4 The ULH structure is formed in the fringe field switching electrode configuration. Note: 20μm scale bar (the inserted photo in 200μm scale bar). The azimuthal angle β is 0° and 45° for (a) and (b) respectively.

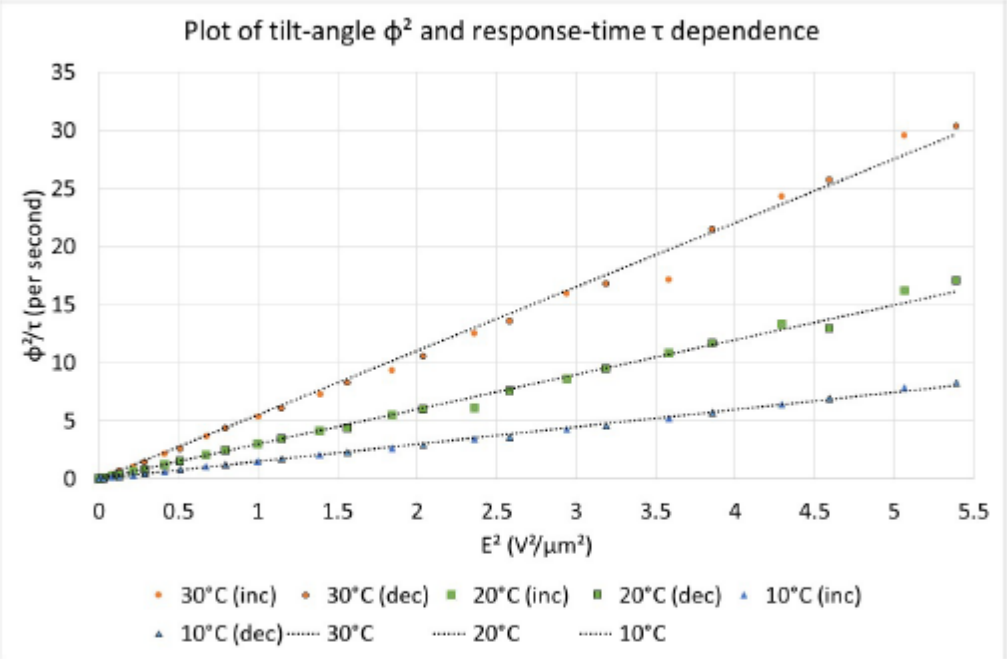

Fig. 5 Plot of dependence on tilt angle and response time as a function of square of electric field at different temperature. The device in the transverse field switching electrode configuration was used for the measurements. Note: 10°C (Triangle), 20°C (Square) and 30°C (Circle).

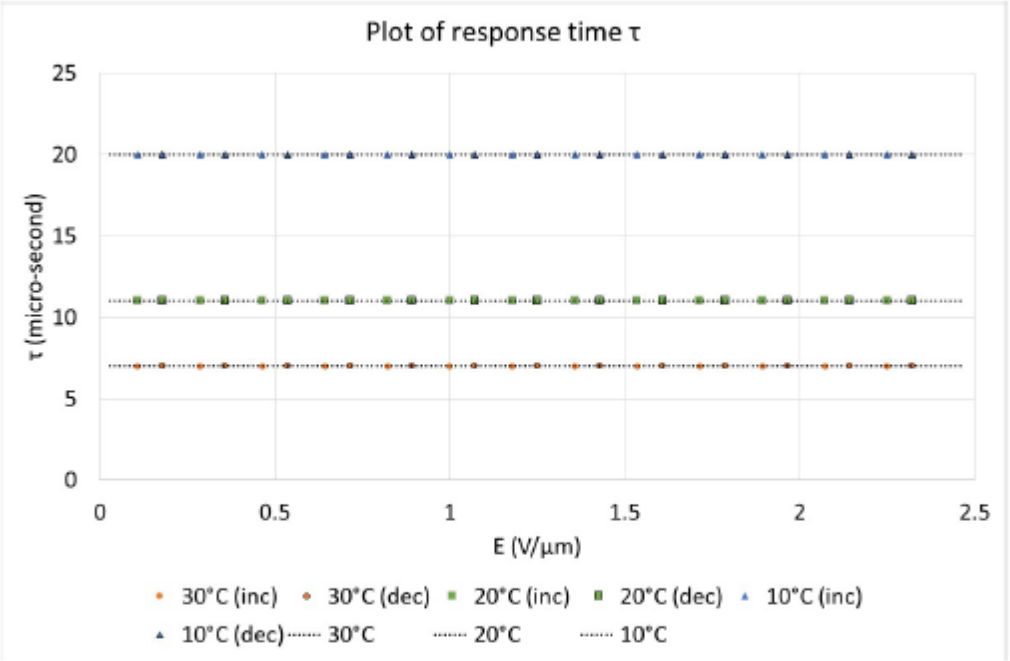

Fig. 6 Plot of response time as a function of electric field at different temperature. The device in the transverse field switching electrode configuration was used for the measurements. Note: 10°C (Triangle), 20°C (Square) and 30°C (Circle).